

## Supporting Information

### Osmotic Release of Drugs via Deswelling Dynamics of Microgel: Modeling of Collaborative Flow and Diffusions

Jize Sui

State Key Laboratory of Nonlinear Mechanics, Institute of Mechanics, Chinese Academy of Sciences, Beijing 100190, China

#### I: Apparent diffusion coefficient matrix

Using Einstein's relation, as discussed in the main text, the friction coefficients of the nanoparticle relative to water and the gel network are given by  $\xi_{cw} = k_B T / D_{cw}$  and  $\xi_{cp} = k_B T / D_{cp}$ , where  $D_{cw}$  and  $D_{cp}$  are the diffusivities of the nanoparticle in water and in polymer network (percolated solid), respectively. We consider here  $D_{cw}$  as a constant at a certain temperature 36 °C, while the diffusivity  $D_{cp}$  is generally associated with the percolated nature of crosslinked polymer network and can be complicated. As the microgel shrinks, the polymeric network displays a compressible deformation, leading to an increasing concentration of entangled polymers in the bulk, which reduces the average mesh size in the gel network. In consequence, the diffusivity of nanoparticles throughout the deswollen microgel will be significantly altered. In this work, we would like to address such a complexity in  $D_{cp}$  by utilizing the empirical expression suggested by R. Hołyst et al.,<sup>1</sup> yielding

$$\frac{D_{cw}}{D_{cp}} = \exp\left(\frac{R_{eff}}{\zeta}\right)^a, \quad (S1)$$

where the fitting exponent  $a$  is assumed to be a constant of order 1 (whose physical meaning is still under discussion<sup>1</sup>),  $\zeta$  is the correlation length interpreted as the average mesh size in the polymer network, and  $R_{eff}$  is an effective hydrodynamic radius related to the nanoparticle radius  $R_c$  and the gyration radius of a polymer coil  $R_p$  at the reference state. In such a diffusivity model, the correlation length, or the average mesh size, is suggested to be expressed by a simple scaling law as following

$$\zeta = b R_p \phi_p^\beta, \quad (S2)$$

where the pre-factor is assumed to be  $b = 1$ , and the exponent is taken as  $\beta = -0.75$  in a good solvent.<sup>1,2</sup> Eq. S2 indicates that the average mesh size between the entangled polymers increases with an increasing gyration (or hydrodynamic) radius of the polymer coil, while decreases with an increasing polymer concentration. Furthermore,

the effective radius can be conducted by the correlation function  $R_{eff}^{-2} = R_c^{-2} + R_p^{-2}$ , yielding

$$R_{eff} = R_p \left(1 + \left(\frac{\lambda_p}{\lambda_c}\right)^2\right)^{-\frac{1}{2}}, \quad (S3)$$

where  $\lambda_c = R_c/R_w$ ,  $\lambda_p = R_p/R_w$ .

Solving the force balance equations for water and the nanoparticle inside the microgel with condition of zero bulk volumetric flux, Eqs. 1-3 in the main text, we can obtain the average velocities of water and the nanoparticle with respect to the gel network, respectively

$$V_w = d_{11} * \frac{\partial}{\partial r} \left( \frac{\partial \tilde{f}}{\partial \phi_w} \right) + d_{12} * \frac{\partial}{\partial r} \left( \frac{\partial \tilde{f}}{\partial \phi_c} \right), \quad (S4)$$

$$V_c = d_{21} * \frac{\partial}{\partial r} \left( \frac{\partial \tilde{f}}{\partial \phi_w} \right) + d_{22} * \frac{\partial}{\partial r} \left( \frac{\partial \tilde{f}}{\partial \phi_c} \right), \quad (S5)$$

where  $\tilde{f} = f\sigma_w/k_B T$  is the dimensionless free energy density, and the coefficients are presented as following

$$d_{11} = \frac{5D_{wc}}{Q} \lambda_c^3 \lambda_p^2 \phi_w^5 (1 - \phi_w - \phi_c)^{2\beta} \left( 1 + e^{\frac{(1 - \phi_w - \phi_c)^{-\beta}}{\sqrt{1 + (\lambda_p/\lambda_c)^2}}} \right), \quad (S6)$$

$$d_{12} = \frac{5D_{wc}}{Q} \lambda_c^3 \lambda_p^2 \phi_c (1 - \phi_w - \phi_c)^{2\beta}, \quad (S7)$$

$$d_{21} = \frac{5D_{wc}}{Q} \lambda_c^3 \lambda_p^2 \phi_w^5 (1 - \phi_w - \phi_c)^{2\beta}, \quad (S8)$$

$$d_{22} = \frac{D_{wc}}{Q} \lambda_c^3 (5\lambda_p^2 \phi_c (1 - \phi_w - \phi_c)^{2\beta} + 4K_g \lambda_c^2 \phi_w^5 (1 - \phi_w - \phi_c)^2), \quad (S9)$$

$Q$

$$= -4K_g \lambda_c^2 \phi_w^5 (1 - \phi_w - \phi_c)^2 - e^{\frac{(1 - \phi_w - \phi_c)^{-\beta}}{\sqrt{1 + (\lambda_p/\lambda_c)^2}}} (5\lambda_p^2 \phi_c (1 - \phi_w - \phi_c)^{2\beta} + 4K_g \lambda_c^2 \phi_w^5 (1 - \phi_w - \phi_c)^2) \quad (S10)$$

In above equations, we have employed the semi-empirical expressions to qualify the permeability of water penetrating through the nanoparticles (obtained by Russel et al. <sup>3</sup>) and the gel network (Carmen-Kozeny expression <sup>2,4</sup>), respectively

$$\kappa_{wc} = \frac{R_c^2 \phi_w^6}{K_c \phi_c}, \quad (S11)$$

$$\kappa_{wp} = \frac{\left(\frac{\zeta}{2}\right)^2 \phi_w}{K_p \phi_p^2}, \quad (S12)$$

where the constant  $K_c = 5$  is often for colloids, while the Kozeny constant for the gel network  $K_p$  should be usually determined by the experimental measurements.

Substituting above set of equations into the fluxes of water  $J_w = \phi_w V_w$  and the nanoparticle  $J_c = \phi_c V_c$ , as represented in Eqs. 6 and 7 in the main text, we can express, therefore, the apparent diffusivity matrix  $D$  mentioned in the main text as following

$$D = \begin{vmatrix} \phi_w (d_{11} \tilde{f}_{ww} + d_{12} \tilde{f}_{wc}) & \phi_w (d_{12} \tilde{f}_{cc} + d_{11} \tilde{f}_{wc}) \\ \phi_c (d_{21} \tilde{f}_{ww} + d_{22} \tilde{f}_{wc}) & \phi_c (d_{22} \tilde{f}_{cc} + d_{21} \tilde{f}_{wc}) \end{vmatrix}, \quad (S13)$$

where  $\tilde{f}_{ww} = \frac{\partial^2 \tilde{f}}{\partial \phi_w^2}$ ,  $\tilde{f}_{cc} = \frac{\partial^2 \tilde{f}}{\partial \phi_c^2}$  and  $\tilde{f}_{wc} = \frac{\partial^2 \tilde{f}}{\partial \phi_w \partial \phi_c}$ . Therefore, the candidates  $D_{ij}$  ( $i, j=1, 2$ )

mentioned in the main text can correspond to the components of the matrix  $D$  as shown in Eq. S13.

## II: Free energy density model

As stated in the main text, the free energy density in the nanocomposite microgel can be simply written as

$$f = f_{mix} + f_{ela} + f_{ext} \quad (S14)$$

The first two items in Eq. S14 have been explained in the main text. Here, we emphatically address the last item, i.e., the extra free energy density  $f_{ext}$ , which consists of two contributions  $f_{ext} = f_{cc} + f_{cp}$  with  $f_{cc}$  accounting for the interparticle interactions and  $f_{cp}$  for the interactions between the nanoparticle and the crosslinked polymer matrix.

$f_{cc}$  can be analytically written as  $f_{cc} = \frac{k_B T}{\sigma_c} \phi_c \int \frac{Z(\phi_c)}{\phi_c} d\phi_c$ , where  $Z(\phi_c)$  is the hard-sphere compressibility as suggested by Carnahan-Starling model <sup>3</sup>

$$Z(\phi_c) = \frac{1 + \phi_c + \phi_c^2 - \phi_c^3}{(1 - \phi_c)^3}, \quad (0 \leq \phi_c \leq 0.55) \quad (S15)$$

Alternatively, the series expansion of the state equation for the hard sphere model with respect to the higher virial coefficient can also achieve the approximate approach. For example, using the summation till the 7<sup>th</sup> virial expansion, we can calculate the formula

$$\sum_{i=2}^7 \frac{B_i}{\sigma_c^i} \phi_c^i, \quad (S16)$$

where the expansion parameter is given by  $B_i = b_i [(2R_c)^3]^{i-1}$  with  $b_i$  being the  $i^{\text{th}}$  virial coefficient as list in Table 1

Table 1: Virial coefficients  $b_i$  for different orders

$b_2$	2.0944	$b_5$	2.1223
$b_3$	2.7415	$b_6$	1.5555
$b_4$	2.6362	$b_7$	1.1647

Accordingly, we can calculate the parameter  $B_i$  as listed in the Table 2

Table 2: Expansion parameters  $B_i$  for different orders

$B_2$	$4\sigma_c$	$B_5$	$28.2366\sigma_c^4$
$B_3$	$10\sigma_c^2$	$B_6$	$39.5255\sigma_c^5$
$B_4$	$18.3646\sigma_c^3$	$B_7$	$56.5226\sigma_c^6$

$f_{cp}$  is analytically expressed as

$$f_{cp} = \frac{k_B T}{\sigma_p} \phi_p \ln \frac{\phi_p}{\alpha(\phi_c)}. \quad (S17)$$

In Eq. S17, the so-called free volume fraction  $\alpha(\phi_c)$  is expressed in the formula as suggested by Lekkerkerker et al.<sup>5-7</sup>

$$\alpha(\phi_c) = (1 - \phi_c) \exp(-A\gamma - B\gamma^2 - C\gamma^3), \quad (S18)$$

where  $\gamma = \phi_c/(1 - \phi_c)$ . The quantities  $A$ ,  $B$  and  $C$  are the functions of ratio  $\delta = \Delta/R_c$ , where  $\Delta$  is the depletion thickness

$$A = 3\delta + 3\delta^2 + \delta^3, \quad (S19)$$

$$B = \frac{9}{2}\delta^2 + 3\delta^3, \quad (S20)$$

$$C = 3\delta^3. \quad (S21)$$

The function  $\alpha(\phi_c)$  appears to characterize the excluded volume interactions between the nanoparticle and the polymer coil. It is worth mentioning that such a depletion thickness  $\Delta$ , according to free volume theory, should be modeled in relation to the curvature of crosslinked polymer monomer forming the gel network. Lekkerkerker et al.<sup>5-7</sup> suggested a mean-field expression of  $\Delta$  (scaled by colloid radius  $R_c$ ) which is derived explicitly for the semi-dilute regime and the broad range of size ratio  $R_p/R_c$

$$\frac{\Delta}{R_c} = \left[ 1 + 3.213 \frac{\zeta}{R_c} + 2.09 \left( \frac{\zeta}{R_c} \right)^2 \right]^{\frac{1}{3}} - 1. \quad (S22)$$

In Eq. S22, we have considered that the depletion thickness  $\Delta$  should be polymer-concentration-dependent, indicating that the gyration radius of polymer coil  $R_p$  used in the original model of  $\Delta$  has been now displayed by the correlation length  $\zeta$ , i.e., the mesh size in the polymer network. With above set of equations, the free energy density  $f$  represented in Eq. 5 in the main text can be eventually determined. Fig. S1 shows the depletion layer thickness varying with the gyration radius of polymer coil  $R_p$  and the concentration of polymers  $\phi_p$ . The depletion layer becomes thinner as either the microgel gets stiffer (a decreasing  $R_p$ ) or the polymer concentration increases.

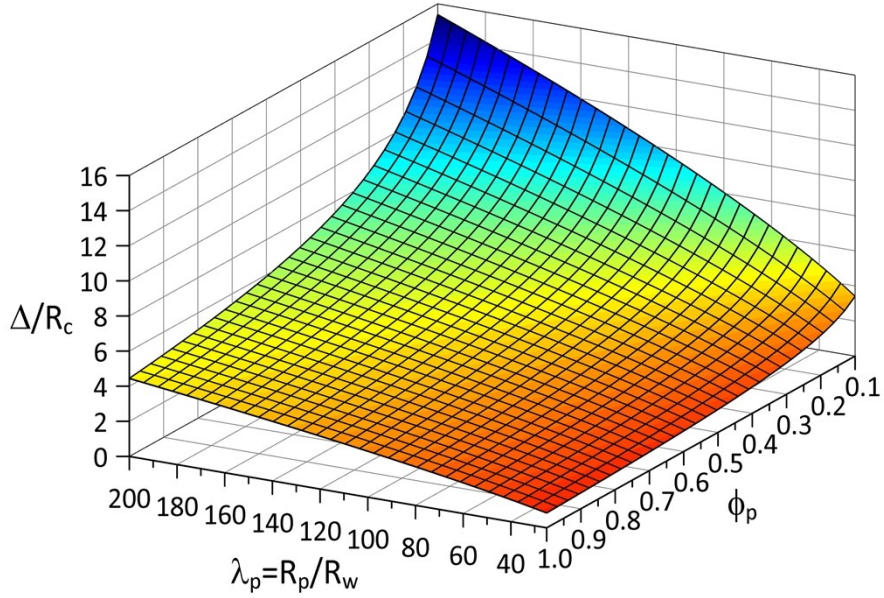


**Fig. S1** Depletion layer thickness is plotted as functions of gyration radius of polymer coil  $R_p$  and concentration of polymers  $\phi_p$  for the nanoparticle with  $R_c = 5$  nm.

### III: Soft-Cell approach (SCA) with dimensionless procedure

SCA is developed on the basis of Lagrangian framework, and is capable of addressing the gel dynamics involving the coexistence of multi-components diffusions and elastic deformation of gel network, as termed diffusio-mechanical coupling (DMC) regime.<sup>8</sup> One outstanding advantage of employing SCA is that the resulting moving interface of the gel materials can be directly determined via the conservation law of the crosslinked polymers (or colloids) retained in the gel instead of solving additional boundary condition which is often derived with a complex function of the multi-components' concentrations.

In short, the employment of SCA can not only enable a dynamic modeling framework to read elegantly, but also achieve the convenience in performing the numerical procedures. Such an approach has been invoked to solve the sedimentation dynamics of the colloidal gel materials in our previous work.<sup>9</sup>

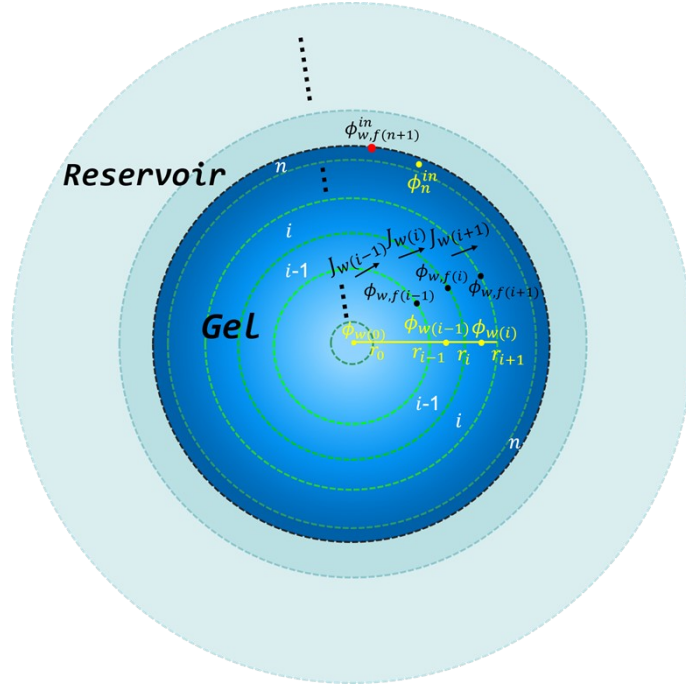


**Fig. S2** Schematic illustration of SCA by taking the diffusive flux of water component for example (the nanoparticle component follows the same procedure). Water, as well as the nanoparticles, diffuses outside the microgel towards the reservoir, and the diffusive flux relative to the crosslinked network has been guided by black arrow.  $\phi_{w(i)}$  and  $\phi_{w,f(i)}$  are the concentrations at the master node in the center of cell  $i$  and at the face of cell  $i$ , respectively.

The SCA is implemented by conducting the dimensionless process for the governing equations by invoking the simple variables as following

$$\tilde{r} = \frac{r}{R_0}, \quad \tau = t \frac{D_{cw}}{R_0^2}, \quad (S23)$$

where  $R_0$  is the initial radius of the fully swollen microgel, and the dimensionless variable  $\tilde{r}$  inside the microgel meets  $0 \leq \tilde{r} \leq 1$ . We consider a swollen microgel with size  $300 \mu\text{m}$ , i.e.,  $R_0 = 150 \mu\text{m}$ , for all the calculations.

Consider 1-D configuration, as shown in Fig. S2, we first divide the domain ranging from the center to the border of the microgel into  $n$  cells with the uniform size, i.e., the concentric circular shells with a width per shell  $\Delta\tilde{r}_{0(i)} = 1/n$  (the gel domain has been scaled by the initial radius  $R_0$ ). Water flux and the nanoparticle flux proceed across every cell as the microgel shrinks, while the polymer concentration occupying in each cell is conserved. As a result, the width of the cell  $i$  at the current state of time  $\tau$  is updated by  $\Delta\tilde{r}_i$ .

As seen in Fig. S2 for the cross-section of the concentric circular shells, the current cell  $i$  has two faces located by point  $\tilde{r}_i$  (left) and  $\tilde{r}_{i+1}$  (right), and has also two sorts of concentrations: the one at the master node  $\phi_{w(i)}$  which occupies in the cell  $i$ , and another one locates at the configured nodes, such as  $\phi_{w,f(i)}$  at the left face and  $\phi_{w,f(i+1)}$

at the right face. Based on the derivations in the main text, the fluxes of water and the nanoparticle across the current face  $i$  are given by

$$J_{w(i)} = D_{11} \frac{\partial \phi_w}{\partial \tilde{r}} \Big|_i + D_{12} \frac{\partial \phi_c}{\partial \tilde{r}} \Big|_i, \quad (S24)$$

$$\tilde{J}_{c(i)} = \tilde{D}_{21} \frac{\partial \phi_w}{\partial \tilde{r}} \Big|_i + \tilde{D}_{22} \frac{\partial \phi_c}{\partial \tilde{r}} \Big|_i, \quad (S25)$$

where the dimensionless fluxes are obtained by  $\tilde{J}_{w(i)} = \frac{R_0}{D_{cw}} J_{w(i)}$  and  $\tilde{J}_{c(i)} = \frac{R_0}{D_{cw}} J_{c(i)}$ , and the dimensionless diffusivity candidates are produced from the apparent diffusivity matrix  $D$  by  $\tilde{D}_{ij} = D_{ij}/D_{cw}$  ( $i, j = 1, 2$ ).

The concentrations of water and the nanoparticle involved in the  $D_{ij}$  ( $i, j = 1, 2$ ) in Eqs. S24 and S25 should be the value at the face  $i$ , i.e.,  $\phi_{w,f(i)}$  and  $\phi_{c,f(i)}$ . These concentrations at the face  $i$  can be approximately determined by the linear interpolation of the concentration at the master nodes in the neighboring cells  $i-1$  and  $i$ , yielding

$$\phi_{w,f(i)} = \frac{\Delta \tilde{r}_{i-1} \phi_{w(i)} + \Delta \tilde{r}_i \phi_{w(i-1)}}{\Delta \tilde{r}_{i-1} + \Delta \tilde{r}_i}, \quad (S26)$$

$$\phi_{c,f(i)} = \frac{\Delta \tilde{r}_{i-1} \phi_{c(i)} + \Delta \tilde{r}_i \phi_{c(i-1)}}{\Delta \tilde{r}_{i-1} + \Delta \tilde{r}_i}. \quad (S27)$$

Moreover, the concentration gradients over the face  $i$  in Eqs. S24 and S25 can be given by the simple differential rule

$$\frac{\partial \phi_w}{\partial \tilde{r}} \Big|_i = \frac{\phi_{w(i)} - \phi_{w(i-1)}}{(\Delta \tilde{r}_i + \Delta \tilde{r}_{i-1})/2}, \quad (S28)$$

$$\frac{\partial \phi_c}{\partial \tilde{r}} \Big|_i = \frac{\phi_{c(i)} - \phi_{c(i-1)}}{(\Delta \tilde{r}_i + \Delta \tilde{r}_{i-1})/2}. \quad (S29)$$

We can subsequently solve the time evolution equations of water and the nanoparticle with respect to the current cell  $i$  at the current state  $\tau_+ = \tau + \Delta\tau$  with the time interval  $\Delta\tau$

$$\phi_{w(i)}(\tau_+) = \phi_{w(i)}(\tau) + 3\Delta\tau \frac{\tilde{J}_{w(i)} \tilde{r}_i^2(\tau_+) - \tilde{J}_{w(i+1)} \tilde{r}_{i+1}^2(\tau_+)}{\tilde{r}_{i+1}^3(\tau_+) - \tilde{r}_i^3(\tau_+)}, \quad (S30)$$

$$\phi_{c(i)}(\tau_+) = \phi_{c(i)}(\tau) + 3\Delta\tau \frac{\tilde{J}_{c(i)} \tilde{r}_i^2(\tau_+) - \tilde{J}_{c(i+1)} \tilde{r}_{i+1}^2(\tau_+)}{\tilde{r}_{i+1}^3(\tau_+) - \tilde{r}_i^3(\tau_+)}. \quad (S31)$$

Herein, as the deswelling proceeds, the width  $\Delta \tilde{r}_i = \tilde{r}_{i+1} - \tilde{r}_i$  of cell  $i$  must alter over time, meaning the ‘‘Soft-Cell’’ nature which differs from the conventional finite volume method, and the variation in size of current cell is determined by the conservation law of the crosslinked polymers retained in the cell  $\Delta \tilde{r}_i$  with respect to

that in the initial cell  $\Delta\tilde{r}_{0(i)}$

$$(\tilde{r}_{i+1}^3 - \tilde{r}_i^3)\phi_{p(i)}(\tau_+) = (\tilde{r}_{0(i+1)}^3 - \tilde{r}_{0(i)}^3)\phi_{p0}, \quad (S32)$$

where  $\phi_{p(i)}(\tau_+) = 1 - \phi_{w(i)}(\tau_+) - \phi_{c(i)}(\tau_+)$  and  $\phi_{p0}$  are the polymer concentrations at the current state and the initial state, respectively. Note that, all the variables at right side of Eq. S32 are the constants initially assigned, and particularly the first cell ( $i = 1$ ) has been regarded as a complete sphere instead of the spherical shell ( $i > 1$ ), hence the conservation law applied to this cell ( $i = 1$ ) reads  $\tilde{r}_1^3\phi_{p(1)} = r_{0(1)}^3\phi_{p0}$  with  $\phi_{p(1)} = 1 - \phi_{w(1)} - \phi_{c(1)}$ .

Performing the time iteration calculations using above set of equations, i.e., the SCA, with the appropriate boundary conditions discussed in the main text, we can produce three desirable spatiotemporal variables  $\phi_w(\tau, \tilde{r})$ ,  $\phi_c(\tau, \tilde{r})$  and  $\tilde{r}_n(\tau) = R(\tau)/R_0$  simultaneously. As discussed earlier, the condition of moving microgel border  $R(t)$  can be directly accessed by  $d\tilde{r}_n(\tau)/d\tau$  in which the elastic deformable behaviors of the bulk microgel and multi-diffusions behaviors are both involved.

In addition, in our framework, the buffer release domain (BRD) has been considered to be a rationalized approach to avoid the demerit of ‘‘perfect sink condition’’ in the existing theories.<sup>10-13</sup> As discussed in the main text, the governing equation in the BRD is a standard diffusion type to characterize the diffusion behavior of the nanoparticles towards the periphery of the BRD. Since the gels is absent in the ambient media, so, technically, we apply a normal scaling criterion upon the diffusion equation instead of SCA route by introducing the following dimensionless variables

$$\tilde{r}_- = \frac{r_- - (R_\infty - H)}{H}, \quad \tau = t \frac{D_{cw}}{R_0^2}. \quad (S33)$$

where  $R_\infty = 2R_0$  is assumed to be the periphery of the BRD, beyond which it is in absence of nanoparticles, and  $r_-$  is the coordinate in the BRD, meeting  $R(t) \leq r_- \leq R_\infty$ , in consequence,  $\tilde{r}_-$  varies in range  $0 \leq \tilde{r}_- \leq 1$ , and  $H(t) = R_\infty - R(t)$  is a time-dependent variable.

Hence, we can write the diffusion equation Eq. 9 in the main text into its dimensionless form

$$\frac{\partial C_{buf}}{\partial \tau} + \frac{\partial C_{buf}}{\partial \tilde{r}_-} \frac{1 - \tilde{r}_- - \partial H}{H} = \frac{1}{\omega H^2} \left( \frac{2H}{\tilde{r}_- H + m - H} \frac{\partial C_{buf}}{\partial \tilde{r}_-} + \frac{\partial^2 C_{buf}}{\partial \tilde{r}_-^2} \right), \quad (S34)$$

where  $\omega = D_{cw}/D_{buf} = \eta_{buf}/\eta_w$  with  $\eta_{buf}$  being the viscosity of the fluid in the BRD, and

$H = H/R_0$  is a dimensionless variable. Here, we assume  $R_\infty = 2R_0$ , hence  $H = 2 - R(\tau)/R_0$ .



It is indicated that the BRD equivalently expands at the same rate at which the microgel shrinks, namely, the time-dependent variable  $H$  used in Eq. S34 can share the same information from the deswollen microgel determined by the SCA at every compute time interval  $\Delta\tau$ . Therefore, such a dimensionless diffusion equation can be solved by using a regular finite differential algorithm.

The dimensionless boundary conditions corresponding to the original ones stated in the main text for our problems are listed as following:

(i):  $\left. \frac{\partial \phi_w}{\partial \tilde{r}} \right|_{i=1} = \left. \frac{\partial \phi_c}{\partial \tilde{r}} \right|_{i=1} = 0$  at the first cell  $\tilde{r}_1$ , meaning the zero fluxes at the center of microgel;

(ii):  $C_{buf} = 0$  at the periphery of the BRD,  $\tilde{r}_- = 1$ ;

(iii): The polymer network at the microgel border  $\tilde{r}_n(\tau)$  remains a deswelling equilibrium state, which indicates an equality in the chemical potentials of water inside and outside the microgel  $\mu_w(\phi_w, \phi_c) = \mu_0$ , i.e.,  $\partial \tilde{f} / \partial \phi_w = \tilde{\mu}_0$  with  $\tilde{\mu}_0 = \mu_0 / k_B T$  being the dimensionless value of chemical potential of water in the ambient media. Here, we assume such a dimensionless value  $\tilde{\mu}_0 = -0.4$  corresponding to the relative viscosity of the plasma in the ambient media  $\omega = \eta_{buf} / \eta_w = 2.4$ .

(iv): Equality in the concentrations and the diffusion fluxes between the microgel and the ambient media at the shrinking microgel border, namely,

$$\phi_{c,f(n)}(\tilde{r}_n(\tau), \tau) = C_{buf}(\tilde{r}_- = 0, \tau) \text{ and } -\mathcal{J}_{c(i)}(\tilde{r}_n(\tau), \tau) = \frac{1}{\omega \tilde{H}} \left. \frac{\partial C_{buf}}{\partial \tilde{r}_-} \right|_{\tilde{r}_- = 0} - \frac{\partial H}{\partial \tau} C_{buf}(\tilde{r}_- = 0, \tau).$$

#### IV: Some supplementary results

According to the force balance equations (2) and (3) in the main text, we can obtain the total friction coefficients of water and the nanoparticles when they diffuse outside the microgel

$$\begin{aligned} \tilde{\xi}_w &= \tilde{\xi}_{wc} + \tilde{\xi}_{wp} \\ &= \sigma_w \eta_w \left( \frac{1}{\kappa_{wc}} + \frac{1}{\kappa_{wp}} \right) \\ &\cong \sigma_w \eta_w \left( \frac{K_c}{R_c^2} + \frac{4K_g}{R_p^2} \right), \end{aligned} \quad (S35)$$

$$\begin{aligned} \tilde{\xi}_c &= \tilde{\xi}_{cw} + \tilde{\xi}_{cp} \\ &= \frac{k_B T}{D_{cw}} \left( 1 + \frac{D_{cw}}{D_{cp}} \right). \end{aligned} \quad (S36)$$

Then, using Einstein relationship, the bulk diffusivities of water and the

nanoparticles are expressed as  $\bar{D}_{wg} = k_B T / \xi_w$  and  $\bar{D}_{cg} = k_B T / \xi_c$ , and their ratio is obtained as

$$\frac{D_{wg}}{D_{cg}} = \frac{4.5 \lambda_c}{\left(\frac{K_c}{\lambda_c^2} + \frac{4K_g}{\lambda_p^2}\right)} \left(1 + \exp\left(\frac{\left(1 + \left(\frac{\lambda_p}{\lambda_c}\right)^2\right)^{-0.5}}{\phi_p^{-0.75}}\right)\right), \quad (S37)$$

where the constant for nanoparticle is  $K_c = 5$ . The Kozeny constant  $K_g$  for the gel network can be a large number generally obtained by experimental measurements.

Here, we simply evaluate  $K_g = 5.5 \times 10^5$  by setting the diffusivity ratio  $D_{wg}/D_{cg} \approx 1$  for the moderate microgel with  $R_p = 20$  nm and the nanoparticle size  $R_c = 5$  nm (i.e.,  $\lambda_p = 100$  and  $\lambda_c = 25$ ).

As stated in the main text, the intrinsic elastic modulus of the microgel at the reference state, i.e., the collapsed state, is given by  $G_0 = m k_B T / \sigma_p$  with the binding effect  $m = 100$  and the unit volume of polymer coil  $\sigma_p = 4\pi R_p^3 / 3$ . At the temperature 36 °C, we show the relationship between the gyration radius of polymer coil  $R_p$  and the intrinsic elastic modulus  $G_0$  in Fig. S3.

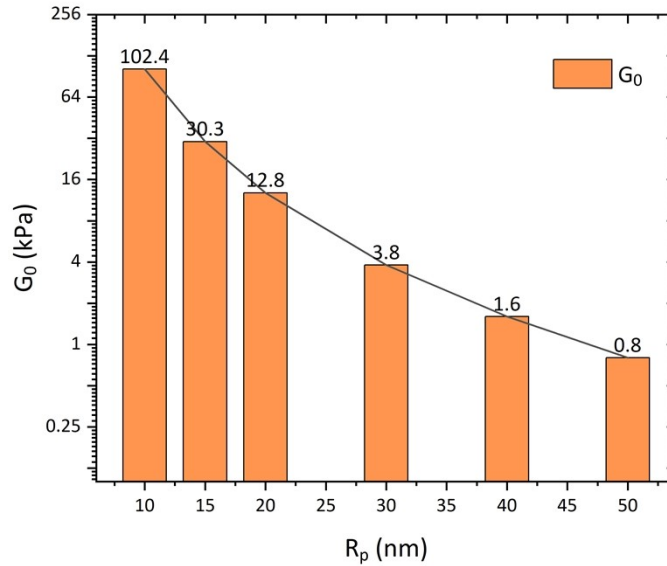


**Fig. S3** The intrinsic elastic modulus  $G_0$  is plotted versus the gyration radius of polymer coil  $R_p$  at the collapsed state of the microgel.

We compare the release dynamics between the U-MG and the F-MG in Fig. S4. As one can see, these two sorts of microgel display the different release behaviors in both cumulative release fraction and BRD-averaged concentration of the nanoparticle at the stages ranging from the earlier to the medium deswelling process, while they shear almost the same release behaviors at the later state of deswelling until the

deswelling equilibrium. As we expected, the F-MG exhibits the better performance in releasing the drugs than the U-MG since the polymers crosslink sparsely with the larger average mesh size in the fuzzy corona regime, which enables the higher efficiency for the drugs passing through the gel network.

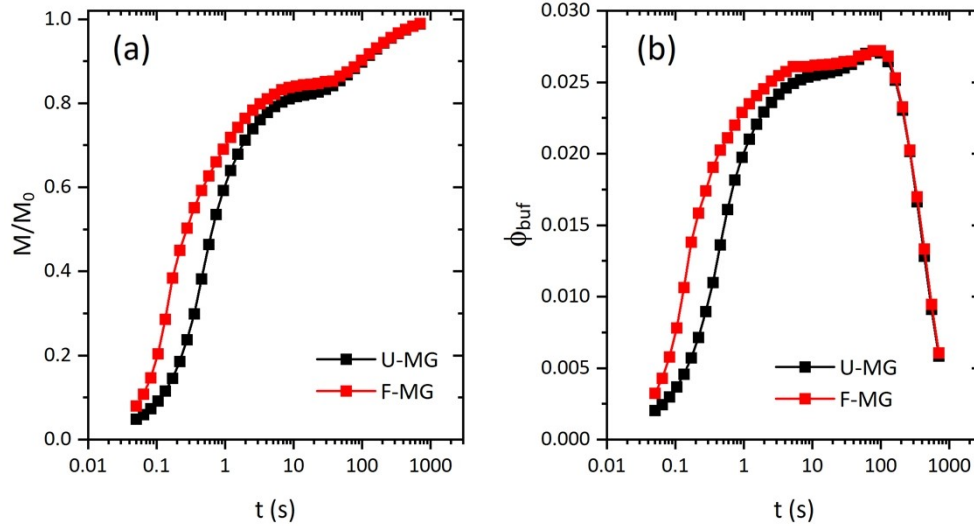


**Fig. S4.** Comparisons of dynamics release behaviors (a) cumulative release fraction and (b) BRD-averaged concentration of drugs between the uniform microgel and the fuzzy microgel. Parameters used here are  $K_g = 5.5 \times 10^5$ ,  $G_0 = 12.8$  kPa,  $R_c = 5$  nm,  $\omega = 2.4$ ,  $\bar{\mu}_0 = -0.4$ .

## References

- 1 T. Kalwarczyk, N. Ziębacz, A. Bielejewska, E. Zaboklicka, K. Koynov, J. Szymański, A. Wilk, A. Patkowski, J. Gapiński, H.-J. Butt and R. Hołyst, *Nano Lett.*, 2011, **11**, 2157.
- 2 T. Bertrand, J. Peixinho, S. Mukhopadhyay and C. W. MacMinn, *Phys. Rev. Applied*, 2016, **6**, 064010.
- 3 S. S. L. Peppin, J. A. W. Elliott and M. G. Worster, *J. Fluid Mech.*, 2006, **554**, 147.
- 4 R. W. Style and S. S. L. Peppin, *Proc. R. Soc. A*, 2011, **467**, 174.
- 5 H. N. W. Lekkerkerker, W. C.-K. Poon, P. N. Pusey, A. Stroobants and P. B. Warren, *Europhys. Lett.*, 1992, **20**, 559.
- 6 D. G. A. L. Aarts, R. Tuinier and H. N. W. Lekkerkerker, *J. Phys.: Condens. Matter*, 2002, **14**, 7551.
- 7 R. Tuinier, D. G. A. L. Aarts, H. H. Wensink and H. N. W. Lekkerkerker, *Phys. Chem. Chem. Phys.*, 2003, **5**, 3707.
- 8 M. Doi, *Soft Matter Physics* (Oxford University Press, Oxford, 2013).
- 9 J. Z. Sui, *Phys. Chem. Chem. Phys.*, 2020, **22**, 14340.
- 10 L. Serra, J. Doménech and N. A. Peppas, *Biomaterials*, 2006, **27**, 5440.
- 11 K. Vulic, M. M. Pakulska, R. Sonthalia, A. Ramachandran and M. S. Shoichet, *J. Control. Release*, 2015, **197**, 69.
- 12 J. A. Maroto-Centeno and M. Quesada-Pérez, *J. Chem. Phys.*, 2020, **152**, 024107.

13 F. M. Kashkooli, M Soltani and M. Souri, J. Control. Release, 2020, **327**, 316.